J. Membrane Biol. 159, 41–52 (1997)

The Journal of
Membrane
Biology

Concentration Dependence of Sodium Permeation and Sodium Ion Interactions in the Cyclic AMP-gated Channels of Mammalian Olfactory Receptor Neurons

S. Balasubramanian[1], **J.W. Lynch**[2,*], **P.H. Barry**[1]

[1]School of Physiology and Pharmacology, University of New South Wales, Sydney 2052, Australia
[2]Neurobiology Division, Garvan Institute of Medical Research, Darlinghurst, Sydney 2010, Australia

Received: 7 November 1996/Revised: 24 March 1997

Abstract. The dependence of currents through the cyclic nucleotide-gated (CNG) channels of mammalian olfactory receptor neurons (ORNs) on the concentration of NaCl was studied in excised inside-out patches from their dendritic knobs using the patch-clamp technique. With a saturating concentration (100 μM) of adenosine 3′, 5′-cyclic monophosphate (cAMP), the changes in the reversal potential of macroscopic currents were studied at NaCl concentrations from 25 to 300 mM. In symmetrical NaCl solutions without the addition of divalent cations, the current-voltage relations were almost linear, reversing close to 0 mV. When the external NaCl concentration was maintained at 150 mM and the internal concentrations were varied, the reversal potentials of the cAMP-activated currents closely followed the Na^+ equilibrium potential indicating that $P_{Cl}/P_{Na} \approx 0$. However, at low external NaCl concentrations ($\leqslant$100 mM) there was some significant chloride permeability. Our results further indicated that Na^+ currents through these channels: (i) did not obey the independence principle; (ii) showed saturation kinetics with K_ms in the range of 100–150 mM and (iii) displayed a lack of voltage dependence of conductance in asymmetric solutions that suggested that ion-binding sites were situated midway along the channel. Together, these characteristics indicate that the permeation properties of the olfactory CNG channels are significantly different from those of photoreceptor CNG channels.

Key words: Olfactory receptor neuron — Dendritic knob — Cyclic AMP — Cyclic nucleotide-gated channel — Cation permeation — Concentration effects

Present address: Department of Physiology and Pharmacology, The University of Queensland, St. Lucia, Qld 4072, Australia

Correspondence to: P.H. Barry

Introduction

Upon stimulation by odorants there is a G-protein mediated stimulation of either adenosine 3′,5′-cyclic monophosphate (cAMP) or inositol 1,4,5-trisphosphate (IP_3) second messenger systems in olfactory receptor neurons (ORNs) (Boekhoff et al., 1990; Reed, 1992; Ronnet et al., 1993). Cyclic nucleotide-gated (CNG) channels directly activated by cAMP (Nakamura & Gold, 1987) underlie, at least in part, the cationic current responsible for the generation of action potential in the olfactory signal transduction. CNG channels belong to a group of nonselective cation channels directly activated by cyclic nucleotides with diverse functions and tissue distributions (for a review, *see* Finn, Grunwald & Yau, 1996). Olfactory CNG channels, distributed in large numbers in the cilia and the dendritic knob regions of the ORNs, are nonselective cation channels poorly discriminating between monovalent alkali cations, with large minimum pore dimensions of about 6.5 Å × 6.5 Å because of the permeability of tetraethylammonium (TEA) and tris (hydroxymethyl) aminomethane (Tris) (Goulding et al., 1993; Balasubramanian, Lynch & Barry, 1995). In this paper, we have aimed to explore the permeation properties of cation transport through mammalian olfactory CNG channels by recording macroscopic currents across excised membrane patches from the dendritic knobs of olfactory receptor neurons from adult female Wistar rats. The measurements were made with the external membrane surface (pipette) concentrations of NaCl kept constant and the concentration of NaCl on the cytoplasmic side of the membrane being changed. We have endeavored to further characterize the mechanism of permeation through the olfactory CNG channels by examining the ionic dependence of macroscopic currents through excised inside-out patches from dendritic knobs of these olfactory receptor neurons.

Though some experiments on the ion concentration dependence of the *photoreceptor* CNG channel activated by cGMP have been carried out (Furman & Tanaka, 1990; Menini, 1990; Zimmerman & Baylor, 1992; Picones & Korenbrot, 1992; Haynes, 1995; Sesti et al., 1995) much less is known about cation permeation through *olfactory* CNG channel. Despite an extensive amino acid sequence identity with that of its photoreceptor counterpart (Kaupp, 1991) there are already suggestions that the permeation properties are different (Goulding et al., 1993; Balasubramanian et al., 1995). Our present study sought to determine further information about cation permeation through the olfactory CNG channels by recording the changes in the current amplitude and reversal potential observed by following the changes in the internal and external concentrations of NaCl across the dendritic knob membrane patches.

Preliminary results of this work have been published in abstract form (Balasubramanian, Lynch & Barry, 1996).

Materials and Methods

Cell Preparation

Enzymatically dissociated olfactory receptor neurons from adult female Wistar rats were obtained from olfactory epithelial tissue lining the nasal septum and turbinates after quickly killing the rats using CO_2 inhalation. Cell dissociation and isolation techniques were basically the same as those described in detail previously (e.g., Lynch & Barry, 1991; Balasubramanian, Lynch & Barry, 1995). After enzymatic dissociation with trypsin the isolated cells were transferred to the recording chamber where they were continuously superfused with General Mammalian Ringer's (GMR) solution. The dissection and the experiments were performed at room temperature 21 ± 1°C.

Electrophysiological Recording

The CNG channels (activated by cAMP) were studied in excised inside-out patches from the membranes of the dendritic knobs (~1–2 μm in diameter) of isolated olfactory receptor neurons (5–8 μm in diameter) using standard patch-clamp techniques (Hamill et al., 1981). Fire-polished patch pipettes with a tip diameter of about 0.2 μm and resistance of 10–15 MΩ were used to obtain gigaseals on the membrane. Channels were activated by the addition of 100 μM cAMP sodium salt (Sigma Chemical, St. Louis, MO). Patches were excised in the inside-out configuration by brief air exposure. Currents were measured using an Axopatch-ID amplifier (Axon Instruments, Foster City, CA). The current signal was filtered at 2 kHz and digitized at a sampling interval of 0.1 msec, monitored online and stored on an IBM-compatible 486 computer running pCLAMP software (Axon Instruments, Foster City, CA). This was also sued to control the D/A converter for generation of voltage clamp protocols and analysis of generated data.

Solutions and Perfusion System

The ionic composition of the solution filling the patch pipette was initially (in mM): NaCl 150, ethylene glycol-bis (aminoethylether) N, N, N′ N′-tetraacetic acid (EGTA) 2 and 4-(2-hydroxy-ethyl)-1-piperazineethanesulfonic acid (HEPES) 10 titrated to pH 7.4 with Tris-base. The divalent concentrations in the solutions with 2 mM EGTA resulted in a free [Ca^{2+}] of less than 1 nM (Balasubramanian et al., 1995). The ion composition of the bath solutions and pipette solutions were similar except that in various experiments 150 mM NaCl was substituted with the concentration of NaCl as depicted in the figures and figure legends. Sucrose was added to maintain the osmotic strength of the solutions that were below 150 mM NaCl concentration. In the first series of experiments, cAMP-activated currents were recorded with 150 mM NaCl solution in the pipette when the internal concentrations were changed from 25–300 mM NaCl. In a second series of experiments, the external [NaCl] was maintained at concentrations from 50–250 mM NaCl in the pipette (bathing the outside surface of the membrane patches), while changing the internal concentrations from 50–280 mM NaCl, to compare the currents recorded under different conditions and to assess the symmetrical nature of the channel.

A special multibarrel perfusion system was set up to enable us to change solutions effectively and rapidly across the membrane patches (Balasubramanian et al., 1995). The dissociated olfactory receptor neurons were placed in one compartment of the recording chamber and were continuously superfused by General Mammalian Ringer containing (in mM): NaCl 140, KCl 5, $CaCl_2$ 2, $MgCl_2$ 1, glucose 10 and HEPES 10 (pH 7.4 with NaOH). On-cell patches were obtained among the cilia on the apical knobs of olfactory receptor neurons and excised in inside-out patch configurations by a brief air exposure. A patch-pipette with membrane spanning the tip was then positioned visually in front of the perfusion tubes through which different test solutions flowed. In all the experiments, complete recovery of current was checked by comparing the currents in symmetrical NaCl solutions before and after each concentration of NaCl tested.

Determination of Current-Voltage Relations and Reversal Potentials

The current-voltage relations for the cAMP-activated current and the reversal (zero current) potential, E_{Rev}, were determined under symmetrical and varying NaCl concentrations. An initial set of experiments consisted of 150 mM NaCl on the external side and no added divalent ions, as described in the previous section. The solution bathing the cytoplasmic side of the patch had concentrations of NaCl which ranged from 25–300 mM NaCl. Step-voltage pulses, from a holding potential of 0 mV, increasing and decreasing in steps of 10 mV, from +80 to −70 mV for 180 msec duration were applied both in the presence and absence of 100 μM cAMP. The cAMP-activated currents were obtained from the difference of the recordings in the presence and absence of cAMP. An example of the cAMP-activated currents after background subtraction, in response to step voltage pulses (only responses to 20 mV steps are shown) in various concentrations of NaCl, is shown in Fig. 1.

The average steady-state current was measured and plotted as a function of membrane potential. In all the experiments, the currents and the potentials are represented with the usual sign convention (i.e., the potential of internal with respect to the external membrane surfaces). Because of the nature of the perfusion system, the GMR bath solution would become the effective reference solution, which in turn was connected to the actual reference electrode, which had a similar composition to the GMR (being 140 mM NaCl). The changes in liquid junction potentials, as different solutions were flowed past the membrane patch, would have been generated between the test solution and the GMR bath solution (and would have been generated as if the latter solution were acting as the reference electrode). Thus the composition of GMR was used for the composition of the reference electrode in the

calculations. These liquid junction potential corrections (ranging from +8.4 to −8 mV) were calculated using the updated Windows' version of the software program *JPCalc* (Barry, 1994) and appropriate corrections were applied to the values of membrane potentials. In all cases, the data points in the various graphs represent the average of 3–7 patches and the error bars represent the SEM of those values.

Reversal potentials were obtained by linear interpolation of the currents recorded in response to voltage steps around the reversal potential. The continuous lines to fit the data points for the values of the cAMP-activated current amplitude were obtained using the Goldman-Hodgkin-Katz (GHK_i) current equation (Hille, 1992) given below:

$$I_{Na} = P_{Na} z_{Na}^2 \frac{EF^2}{RT} \frac{[\mathrm{Na}]_i - [\mathrm{Na}]_o \exp(-zFE/RT)}{1 - \exp(-zFE/RT)} \quad (1)$$

where I_{Na} represents the current carried by Na^+ ions, P_{Na} is the Na^+ permeability, E is the membrane potential, $[Na]_i$ and $[Na]_o$ are the activities of Na^+ on the internal and external surfaces of the patch membrane respectively, R is the gas constant, F the Faraday constant, T the absolute temperature and z_{Na} (= 1), the valency of sodium. To fit continuous lines to the data for the current-voltage relations depicted with external surface concentrations of 50 and 100 mM NaCl and various internal concentrations of NaCl, the full current equation had to have, at least in principle, an additional component, I_{Cl}, the current carried by chloride ions due to a finite P_{Cl}/P_{Na}.

Averaged current amplitudes at +50 and at −50 mV under various external NaCl concentrations were plotted as a function of internal NaCl concentration (Fig. 5*A–F*) and the data fitted by a Hill-type equation:

$$I_{Na} = I_{Na,\,max} [\mathrm{Na}]^h / \{[\mathrm{Na}]^h + K_m^h\} \quad (2)$$

where I_{Na} is the current amplitude, [Na] is the concentration of Na^+ bathing the internal surface of the dendritic knob membrane patches, K_m is the dissociation constant and h is the Hill coefficient.

Activity coefficients for the various NaCl concentrations were obtained directly from tables (Robinson & Stokes, 1965) or from the plot of activity coefficients versus known concentrations of NaCl, and the activities were calculated therefrom. Because of the radical variations in ionic strength of the solutions used in these measurements, NaCl activities rather than concentrations were utilized in all the equations used to fit the experimental data points and, as expected, these provided a far better fit than did the use of concentrations.

Results

The primary aim of this paper was to study the effect of changing the internal concentrations of NaCl on the cAMP-activated currents through the CNG channel in the olfactory receptor neurons keeping the external NaCl concentration constant, in order to study the mechanism of cation permeation through the channel.

Currents and reversal potentials were measured under symmetrical NaCl concentrations ranging from 50–250 mM as well as in asymmetrical solutions by changing the internal NaCl concentrations (from 25–300 mM) while keeping the external concentrations of NaCl constant (from 50–250 mM). Initially currents were measured with internal Na^+ at seven different concentrations: 25, 50, 100, 150, 200, 250 and 300 mM with the external Na^+ being kept constant at 150 mM. The same experiment was repeated with external Na^+ kept at concentrations of 50, 100, 200 and 250 mM and changing the internal Na^+ from 50, 100, 150, 200 and 250 or 280 mM. When using concentrations of NaCl lower than 150 mM the solutions were osmotically balanced with sucrose. However at higher concentrations from 200 to 300 mM NaCl the solutions remained hypertonic. The following data thus represent the concentration dependence of the current-voltage relations of cyclic nucleotide gated (CNG) channels activated by cAMP when solutions were changed on either side of the channel.

The Dependence of cAMP-activated Current on Internal Na^+ Concentration

Figure 1*A–C*, shows examples of cAMP-activated currents measured on the same patch with 150 mM NaCl at the outside surface of the membrane with 150, 300 and 50 mM NaCl at the inside surface in response to voltage steps, in increments of 10 mV over the range +80 to −70 mV from a holding potential of 0 mV (the current responses to 20 mV steps are only shown). Figure 2*A–F* shows the amplitude of the steady-state current as a function of membrane potential, corrected for junction potentials from an average of 6 patches including the one shown in Fig. 1. Figure 2 shows that changing the internal NaCl concentration changed both the reversal potential for the cAMP-activated current, which followed E_{Na} closely, and the size of the outward current at positive potentials. Lowering the internal concentration of NaCl shifted the reversal potential in the positive direction while increasing the concentration made the reversal potential more negative. The solid lines in the figure represent the GHK current equation fits to the data normalized for currents at positive potentials. It is seen that the curves deviate at negative potentials indicating that even at negative potentials, where we would expect the currents to be essentially only dependent on the constant pipette concentration, the cAMP-gated currents still vary strongly with the internal concentration and deviate from the GHK current equation predictions. Figures 3 and 4 show examples of average current voltage relations for cAMP-activated currents from 3–7 dendritic knob patches under different concentrations of internal and external NaCl concentrations as indicated in the figures. The striking feature of the graphs is their approximate linearity even in asymmetrical concentration gradients. Though the reversal potential for cAMP-activated currents followed E_{Na} in the case of external 150, 200, 250 mM NaCl (Figs. 2 and 4), there was a deviation in the reversal potential in a more positive direction for the cases of 100 and 50 mM external NaCl (Fig. 3 for 50 mM NaCl, data for 100 mM NaCl *not shown*), indicating a finite Cl^- permeability for these low concentration solutions.

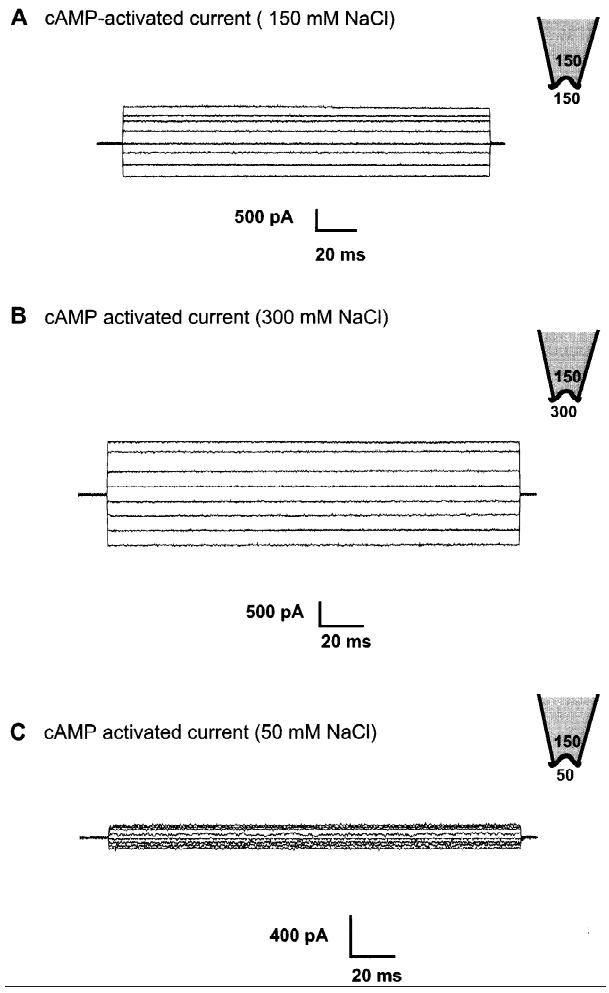

Fig. 1. Ionic dependence of the cAMP-activated currents and current-voltage (*I–V*) relations when the concentration of NaCl bathing the internal surface of inside-out dendritic knob patches from a mammalian olfactory receptor neuron was altered. *A*, *B* and *C* are examples of current through cyclic nucleotide-gated channels activated by 100 μM cAMP, after background subtraction of current traces in the absence of cAMP, in response to voltage pulses of about 180 msec duration, from a holding potential of 0 mV in 10-mV steps (only current responses corresponding to 20-mV steps are shown from +80 mV, lowest trace, to −60 mV, top trace; these voltages were subsequently corrected for liquid junction potentials) as mentioned in Materials and Methods. Current traces are all from the same patch of membrane when the internal concentration of NaCl was varied, as shown in the figures, maintaining the external (pipette) concentration constant at 150 mM.

Currents through the Olfactory CNG Channel Deviate from the Independence Principle

First of all, the saturation of the conductance as the NaCl concentrations are increased clearly violates the independence principle (Hodgkin & Huxley, 1952), an integral assumption for the derivation and validity of the GHK equation in the presence of permeating cations and anions (*see* discussion in Barry & Gage, 1984, for various permeation models in which only ions of one sign are permeating and which give rise to membrane potential equations of similar form to the GHK equation). These results suggest that the flow of the Na^+ ions passing through the channel is limited by ion binding within the channel in clear violation to the independence principle. Figure 5*A–F* shows these saturation effects clearly. The averaged current amplitudes at membrane potentials of +50 and −50 mV were plotted as a function of internal Na^+ concentrations for various external concentrations of NaCl as indicated in Fig. 5 and generally fitted the Hill-type equation (Eq. 2) very well. The only deviation was at small external concentrations where the current values lie above the theoretical fit. Thee parameters used to fit the data points for the example shown in Fig. 5 as well as for the other external concentrations tested are given in the Table. These results show that the Na^+ ions passing through the channel must bind to multiple binding sites within the channel that on an average were occupied half the time when the internal and external Na^+ activity was 113–149 mM at +50 mV and 60 −152 mM NaCl at −50 mV.

Secondly, Figures 2–4 also show that the current-voltage relations for these cAMP-activated currents through olfactory CNG channels under different internal and external NaCl concentrations, deviate from the predictions of the GHK-current equation and indeed, the predictions of other permeation models (*see* e.g., Barry & Gage, 1984), which have the expectation that as the concentration of a permeating ion on one side of the membrane is decreased that will reduce the conductance when current is flowing *from that side* but will not have as much effect when it is flowing *from the other side.* This was clearly not seen to be the case in these measurements.

To investigate the symmetry of the channel, a comparison of data under asymmetrical concentrations was made for both orientations of the membrane. Current-voltage data with 150 mM at the external surface and with concentrations of 50, 100 and 250 mM at the internal surface was compared with the data when the internal surface was 150 mM and the external surface concentrations varied from 50–250 mM. A comparison of the two sets of current-voltage curves is shown in Fig. 6 A–C. The data points with 150 mM NaCl external concentration (in each case fitted with GHKi with 0 permeability for Cl^-; filled circles fitted with continuous lines) were used to compare the data points from different external concentrations of NaCl against the 150 mM NaCl (hollow triangles). It is clear from the graphs that (i) the olfactory CNG channels are considerably symmetrical and that (ii) the cAMP currents through the channels deviate from the independence principle for both membrane orientations.

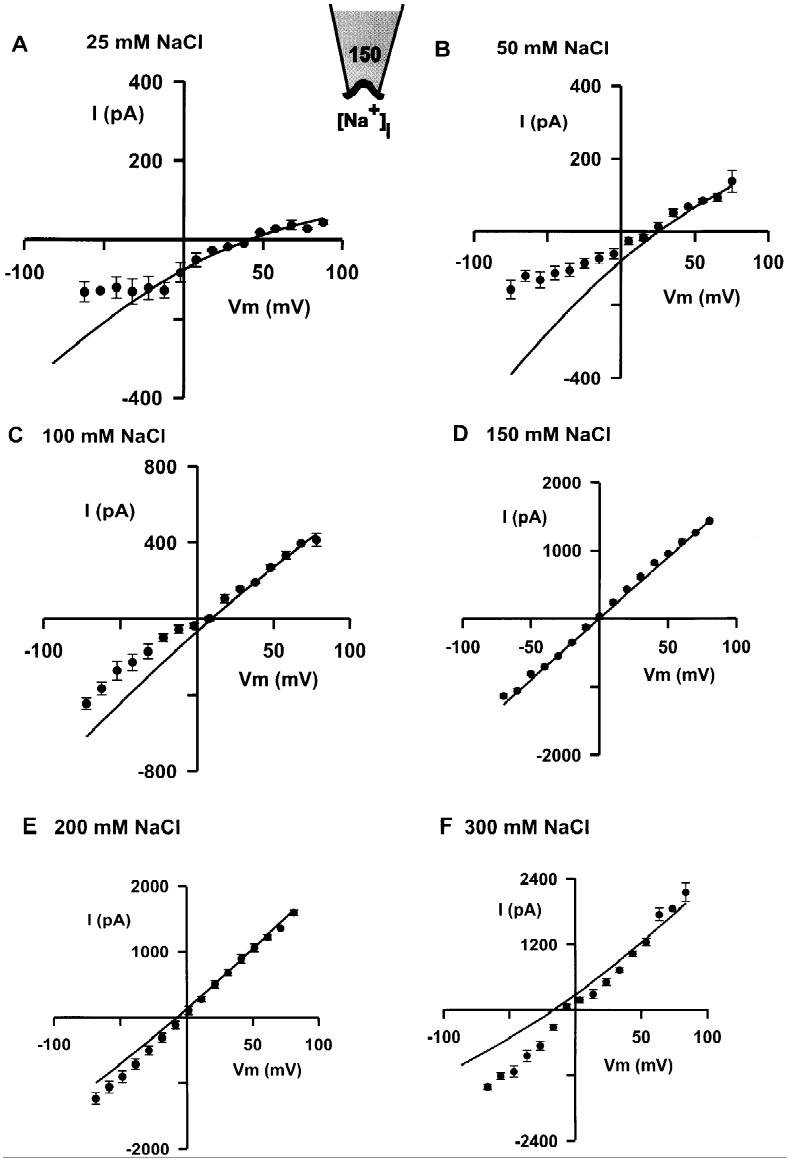

Fig. 2. (*A–F*) Current-voltage relations for olfactory cyclic nucleotide-gated channels (CNG; activated by 100 μM cAMP) when the internal surface concentration of NaCl was changed in the presence of 150 mM NaCl at the outside surface of the inside-out patches from dendritic knobs of olfactory receptor neurons. The reversal potentials for each of the *I–V* curves (*A–F*) were estimated to be +42.9 (25 mM), +20.3 ± 1.5 (50 mM), +8.7 (100 mM), +2.1 ± 1.7 (150 mM), −6.6 (200 mM) and −14 ± 0.5 mV (300 mM) respectively and they are close to the equilibrium potentials of Na^+. The data points represent the average of 6 patches and the error bars indicate the SEM of the values. Continuous lines represent the fit of the outward current data points (from 0 to +80 mV) with GHK current (GHK_i) equation (i.e., Eq. (1)) with the predicted values calculated using ionic activities instead of concentrations, as indicated in Materials and Methods. The deviation from GHK_i fit could be seen for the inward currents for all asymmetrical concentrations of NaCl and clearly the currents through the CNG channels must not obey the independence principle.

Relative Permeability of the Olfactory CNG Channel to Na^+ and Cl^-

The mean reversal potentials (E_{Rev}) from experiments with different external NaCl concentrations were plotted as a function of internal NaCl concentrations (on log scale), as shown in Fig. 7*A–E*. The continuous lines were calculated from the Goldman-Hodgkin-Katz voltage equation using *activities* of ions and assuming the permeability ratio, P_{Cl}/P_{Na} to be 0. The systematic deviation at low Na^+ *activities* could be explained by assuming a finite permeability for Cl^- ions in the GHK-voltage equation. According to this equation (e.g., Hille, 1992), the reversal potential, E_{Rev}, of the current across a membrane or a channel with permeability ratio of chloride and sodium ions P_{Cl}/P_{Na}, defined as p, is given by

$$E_{Rev} = (RT/F) \ln \{([Na^+]_o + p[Cl^-]_i)/([Na^+]_i + p[Cl^-]_o)\} \quad (3)$$

Since Tris base was used to titrate the pH in all the solutions, a factor for Tris permeability ($P_T = P_{Tris}/P_{Na} = 0.65$ from Balasubramanian et al., 1995) was included in the above equation [*see* Eq. (4) below]:

$$E_{Rev} = (RT/F) \ln \{([Na^+]_o + P_T[Tris^+]_o + p[Cl^-]_i)/([Na^+]_i + P_T[Tris^+]_i + p[Cl^-]_o) \quad (4)$$

This correction was especially important at the lower concentrations (e.g., 50 and 100 mM NaCl). The long-

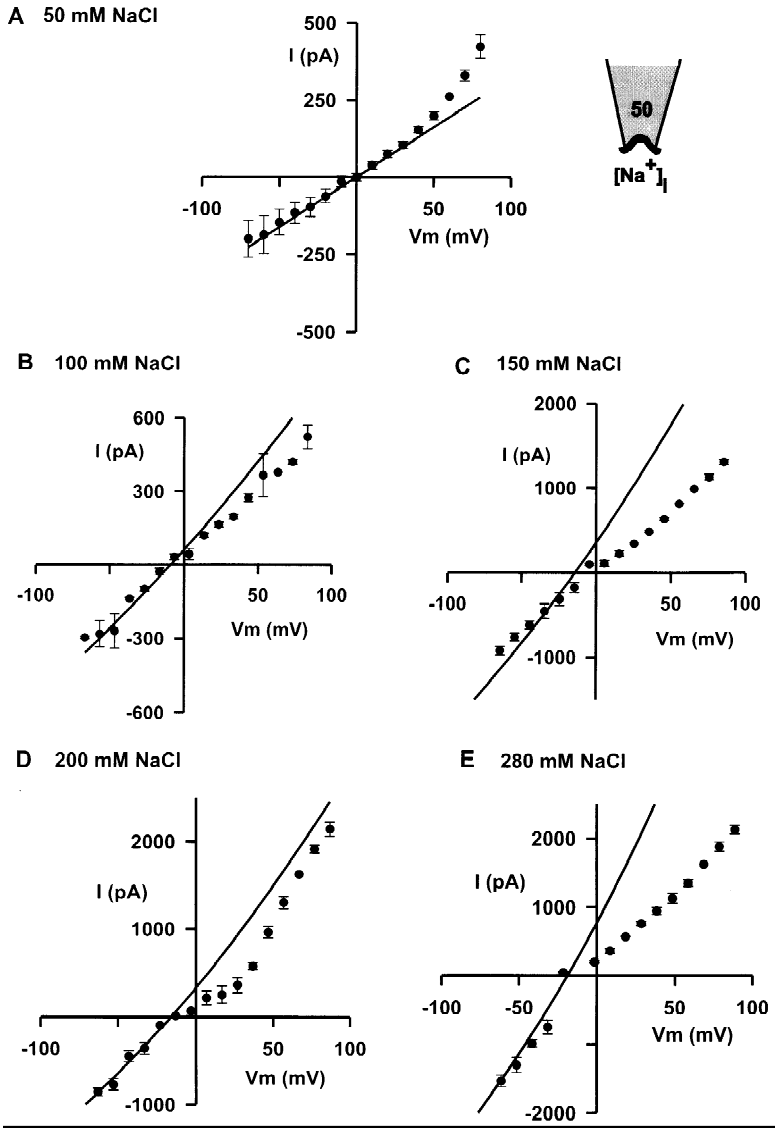

Fig. 3. (*A–E*) Current-voltage (*I–V*) relations for olfactory CNG currents activated by 100 μM cAMP in the presence of 50 mM NaCl at the outside surface (pipette) of inside-out dendritic-knob patches when the internal surface NaCl concentrations were changed as shown in the inset. The data points represent the average of 5–7 patches and the error bars are the SEMs of the values. The continuous lines represent the GHK_i equation, Eq. (1), fit of the inward current data points (from −70 to 0 mV). The reversal potentials for each of the *I–V* curves (*A–E*) were estimated to be −2.6 ± 2.9 (50 mM), −8.9 ± 1.8 (100 mM), −10.6 ± 1.9 (150 mM), −15.9 ± 3.9 (200 mM) and −23.3 ± 1.2 mV (280 mM) respectively. The outward currents (into the pipette) are seen to clearly deviate from the GHK_i predictions.

dashed lines in Fig. 7*A* and *B*, were drawn assuming $p = 0$ and the dotted lines with $p = 0.21$ and $= 0.13$ in Eq. (4), for 50 and 100 mM NaCl respectively. The GHK equation, it should be noted assumes independence and a constant field, may only be used empirically and may not strictly apply in this situation where both cations and anions are permeant (Barry & Gage, 1984), although this is likely to be less of a problem if p is small.

The development of some finite anion permeability at low external NaCl concentrations (e.g., 50 mM or 100 mM) varying internal surface concentrations was somewhat unexpected. We therefore investigated reversal potentials with the opposite orientation of the membrane (internal NaCl concentration at either 50 or 100 mM; with different external concentrations). This necessitated using data from membrane patches from different experiments. In these situations the data could still be fitted using Eq. (4) with a finite chloride permeability, but in this case it was closer to zero than with the other membrane orientation ($P_{Cl}/P_{Na} \approx 0.064$; *graph not shown*).

Discussion

Summary of Results

The aim of these experiments described in this paper was to determine the properties of Na^+ permeation through the cyclic nucleotide-activated channel in excised inside-out patches from dendritic knobs of mammalian olfactory receptor neurons. The results allow a number of conclusions to be reached regarding the structure of the channel and the possible mechanisms of ion transport through it.

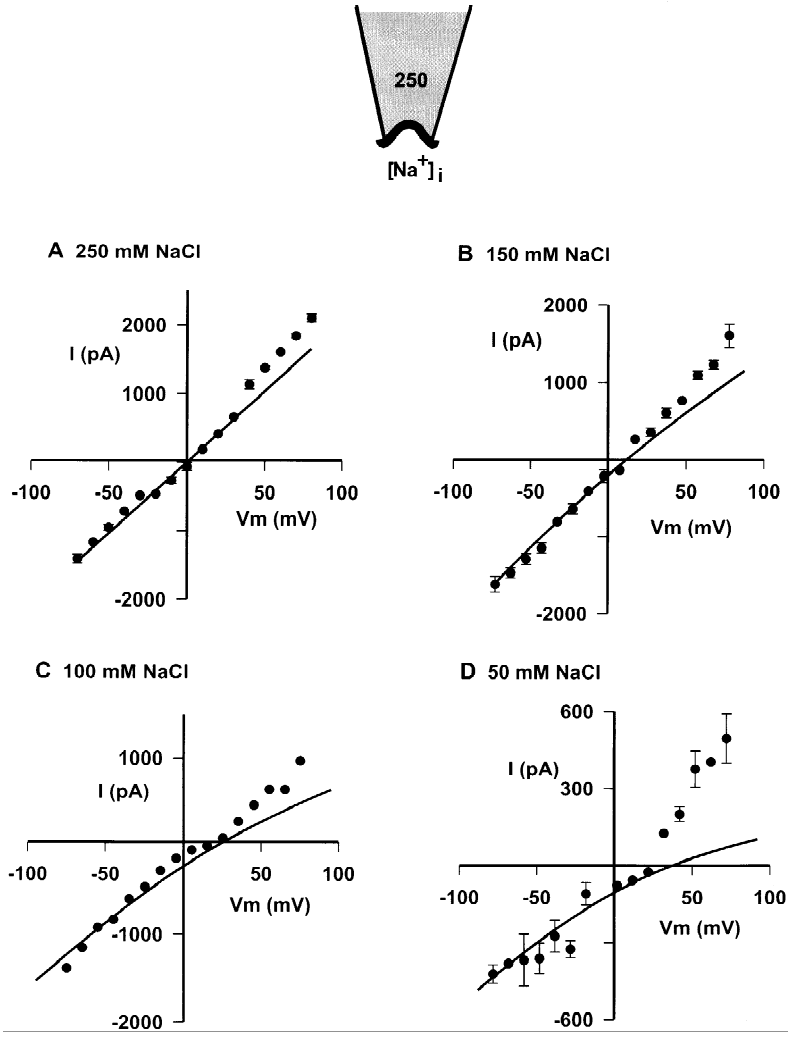

Fig. 4. (*A–D*) Current-voltage (*I–V*) relations for olfactory CNG channels (activated by cAMP) at different internal surface concentrations of NaCl, when the patch pipette contained 250 mM NaCl as shown in the inset. The data points represent the averaged results from 3 inside-out patches and the error bars represent the SEMs of the values. The continuous lines represent the GHK_i equation Eq (1) fit of the inward current data points (from −70 to −10 mV) with $P_{Cl}/P_{Na} = 0$. The changes in the NaCl concentration at the internal surface caused the data points for the outward currents to deviate from the GHK_i predictions. The reversal potentials for the *I–V* curves (*A–D*) were as follows: −1.3 ± 2.5 (250 mM), 10.8 ± 3.1 (150 mM), 21.5 ± 2.6 (100 mM) and 32.1 ± 1.9 mV (50 mM).

The concentration dependence of the current-voltage relations of the olfactory CNG channels was studied in symmetrical NaCl solutions (without added divalent ions), where the current-voltage relations were linear, reversing close to 0 mV. As the NaCl concentration adjacent to the internal surface of the membrane was increased the outward currents began to saturate with dissociation constants between 112–149 mM NaCl. Surprisingly, the inward currents were also dependent on the internal Na^+ activity and exhibited saturation kinetics with an apparent dissociation constant of about 60–152 mM NaCl. cAMP-activated currents through these channels deviated from the predictions of the GHK_i equation (Eq. 1). Saturation of the current is usually also taken as the evidence that the 'independence principle' (i.e., the movement of one ion is not influenced by the movement of other ions) is not valid and that the channel contains at least one binding site (Hille, 1992). Saturation probably results because the ions pass through the channel by binding to specific sites in the channel and hopping from one binding site to the next (Ruff, 1986) and as the concentration in the adjacent solution is increased so all the sites tend to become occupied for most of the time.

When the current-voltage relations from different patches with the same asymmetrical ion concentration gradients but with opposite membrane polarities were plotted on the same graph after normalizing the current values at +50 mV with 150 mM on the external membrane surface with different concentrations on the internal side, it was shown that the data points are virtually, superimposable implying that the CNG channel is fairly symmetrical in nature (Fig. 6*A–C*). The greatest difference was with 50 mM solutions (Fig. 6*A*), where there was a significant shift in E_{Rev} although the overall curves were fairly similar in their slopes and linearity.

The reversal potential closely followed E_{Na} for normal to higher concentrations of NaCl (150, 200 & 250) suggesting a negligible Cl^- permeability (Fig. 7*C, D* and *E*). However the deviations of the reversal potential,

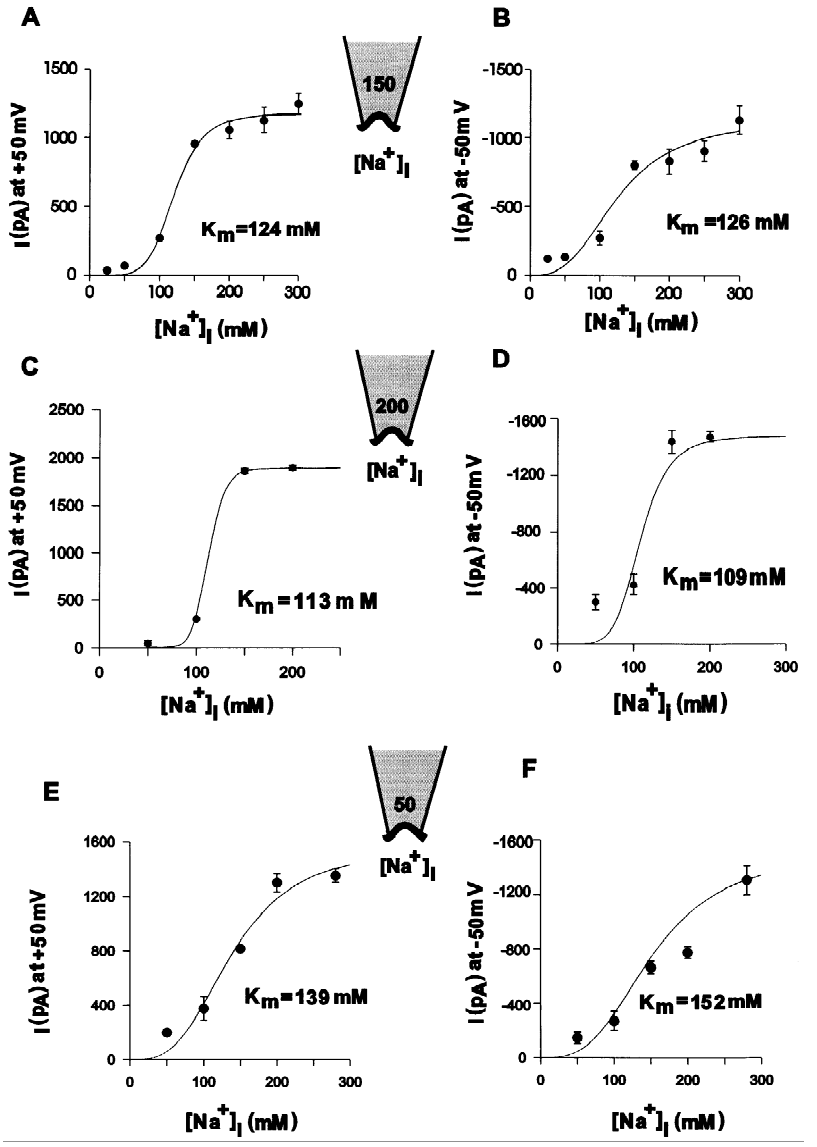

Fig. 5. CNG currents through the cAMP-activated channel from inside-out olfactory dendritic knob patches as a function of the Na^+ concentration at the internal membrane surface. The currents show saturation kinetics in both outward (at +50 mV) and inward (at −50 mV) directions. (*A* and *B*) Averaged cAMP-activated currents at +50 and −50 mV from 5 patches when the external NaCl concentration was 150 mM (data from Figs. 1 and 2), plotted as a function of internal surface concentration of Na^+. The data could be fitted with a Hill type equation Eq. (2), revealing a dissociation constant of 124 mM at +50 mV and 126 mM NaCl at −50 mV. *C* and *D* represent the averaged current data at +50 and −50 mV for an outside surface concentration of 200 mM NaCl (*data not shown*) and *E* and *F* averaged current data for 50 mM NaCl at +50 and −50 mV (from Fig. 3) plotted as a function of internal Na^+ concentration. The continuous lines represent the fit of the data points with a Hill-type equation and the parameters used to fit the equation are given in the Table.

E_{Rev} from E_{Na} for lower external concentrations of 50 and 100 mM NaCl could be explained by the development of a significant anion permeability in the cAMP-activated channel (Fig. 7*A* and *B*). When the lower concentrations of 50 and 100 mM NaCl were maintained at the internal side and the external concentrations varied between 50 to 250 mM, the deviations of the reversal potential (E_{Rev}) from E_{Na} could be fitted with a much lower anion permeability. Though deviations in reversal potentials from E_{Na}, at lower internal NaCl concentrations were observed in CNG channels from rods (Menini, 1990; Zimmerman & Baylor, 1992) and cones (Picones & Korenbrot 1992; Haynes, 1995) and a finite permeability for chloride ions have been suggested, there is no data available for the behaviour of the reversal potentials in the presence of low external NaCl as observed in this paper.

Macroscopic Vs. Single-Channel Measurements

Given that the measurements were made on patches containing hundreds of channels it must be considered whether different types of channels contributed to the response. The small variation in properties from one patch to another would suggest that this population of cAMP-gated channels is uniform. It also seems unlikely that a composite mixture of channel types would have a linear voltage dependence in symmetrical solutions. Since these measurements were done in the absence of Ca^{2+}, Ca^{2+}-gated Cl^- channels would not have a contributed to the currents. In addition, although it is known that the density of CNG channels varies from one region to another, there is no evidence, for example, that extraciliary CNG channels have any different properties

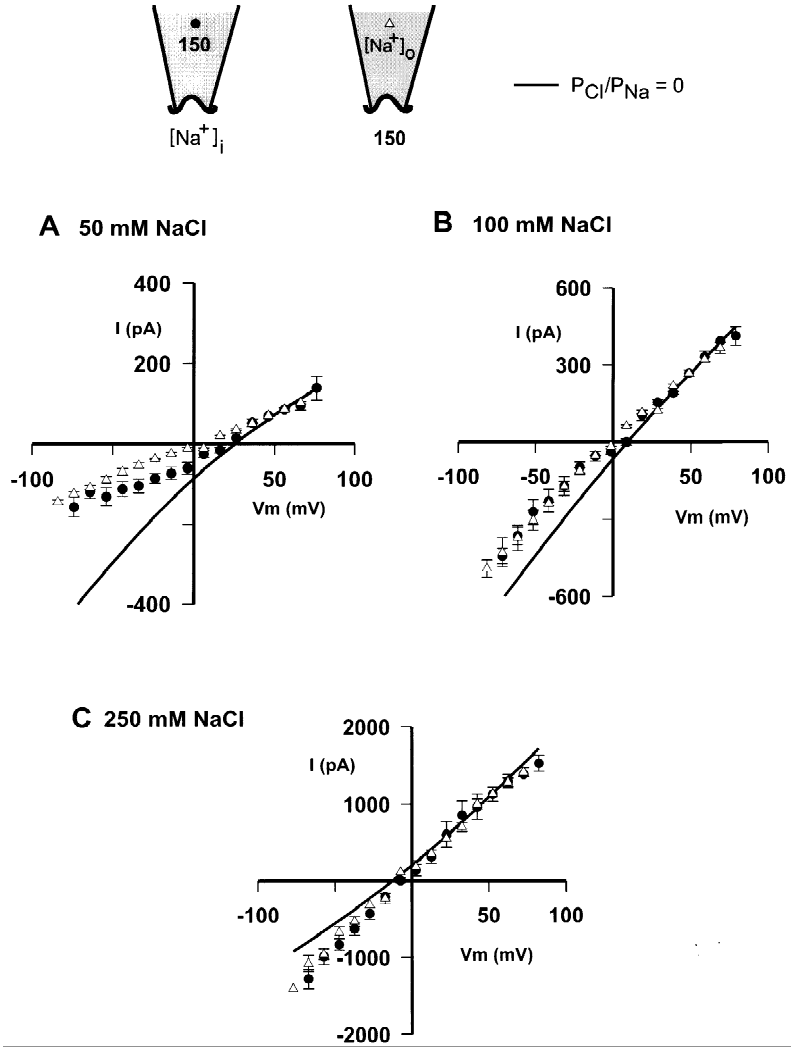

Fig. 6. *A–C* shows a comparison of the same asymmetrical concentration gradient with the opposite configuration of the membrane with data from different patches to assess the symmetrical nature of the olfactory CNG channel. The current-voltage (*I–V*) relations of cAMP-activated currents in the presence of 150 mM NaCl at the external surface of the membrane with 50, 100 and 250 mM NaCl at the internal surface of the inside-out membrane patches are represented by solid circles (data from Fig. 2*B* and *C;* data for 250 mM *not shown*). Data points (hollow triangles) representing normalized current values (normalized in each case to the value at +50 mV in the presence of 150 mM at the external surface) from the experiments with 50 (Fig. 2*C*), 100 (*data not shown*) and 250 mM (Fig. 4*B*) were plotted over the above mentioned *I–V* curves. The signs of the currents were reversed to get the correct representation of asymmetrical gradient with correct orientation of the membrane in each of the cases of normalized current values. Data points are reasonably coincident showing that the olfactory CNG channel is considerably symmetrical. The continuous lines indicate the fit of the outward current data points with the GHK_i equation for $P_{Cl}/P_{Na} = 0$.

from those on the cilia (Firestein, Zufall & Shepherd, 1991; Kurahashi & Kaneko, 1993; Zufall, Firestein & Shepherd, 1991). Another possible problem in measurements of macroscopic currents is the variation in the open-time of the channels with voltage. However, the linear *I–V* relationships, and hence nondependence of conductance, in symmetrical solutions implies that the open-time of the channels is not voltage-dependent under these conditions. This fact together with the stability of currents with time, supports the view that the open-times of the channels in the presence of asymmetrical concentration gradients are also not voltage-dependent. In addition, the reversal potential measurements should be independent of the number of channels that are open at any one time.

Some residual uncertainties may be clarified by single channel measurements. However, such single-channel measurements which will have to be done on the soma of the ORNs are not completely unequivocal as they may have different properties to those localised to the dendritic knobs and cilia of these cells although evidence suggests that they have similar properties (Firestein, Zufall & Shepherd, 1991; Kurahashi & Kaneko, 1993; Zufall, Firestein & Shepherd, 1991).

The linearity of the current-voltage relations in different external NaCl concentrations and the dependence of the inward currents on the internal Na^+ activity imply multiple binding sites in the channel and preliminary modelling with a two-site three-barrier rate theory model (P.H. Barry, *unpublished calculations*) suggests that these ion-binding sites must be located close to the midway point along the channel (Fig. 8). A schematic diagram illustrating this model is shown in Fig. 8. Our results provide information for describing a model for permeation of cations through the olfactory CNG channel.

Comparison with Previous Studies

Deviations from predictions based on the assumption of independent ion movement can provide crucial clues to

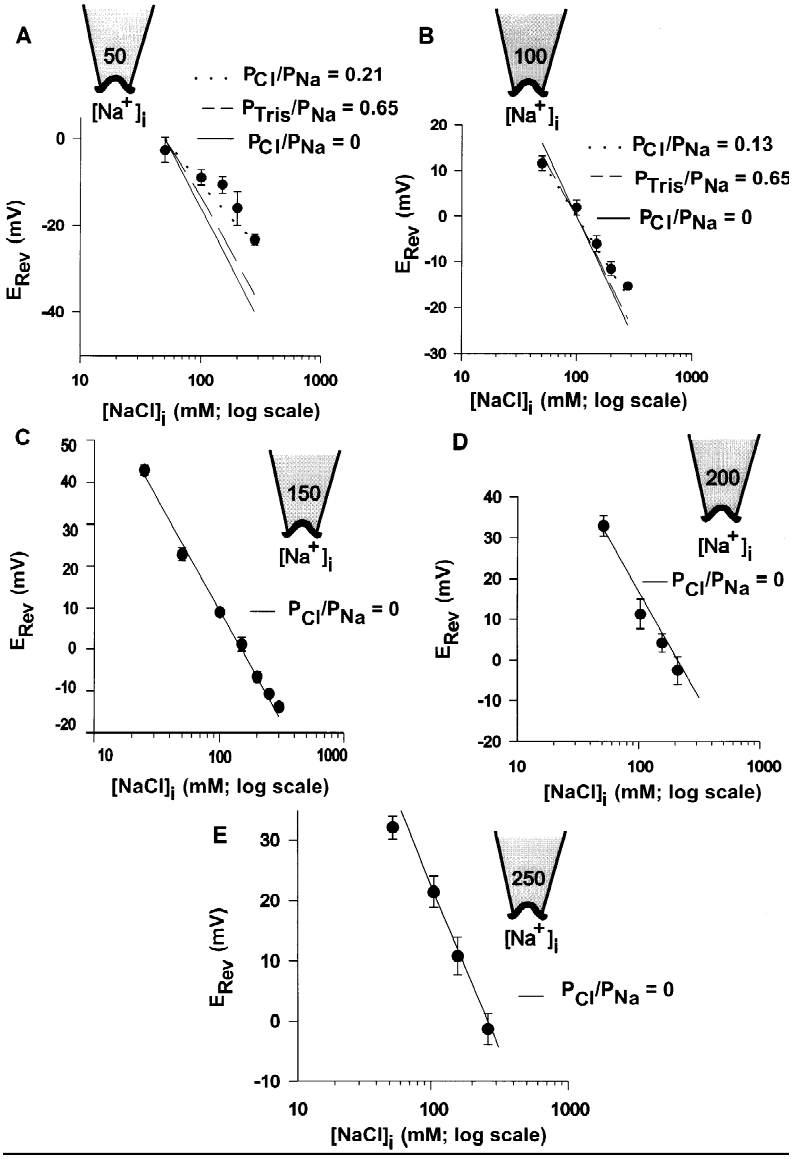

Fig. 7. Dependence of reversal potential of olfactory CNG currents (activated by cAMP) on the internal surface Na^+ concentration. Data points in the graphs *A–E* represent the averaged reversal potentials estimated under different external NaCl concentrations plotted against the internal Na^+ concentration (on a log scale). The continuous lines are calculated from Goldman-Hodgkin-Katz potential equation, Eq. (3), with $P_{Cl}/P_{Na} = 0$, the long dashed lines using Eq. (4) with $P_{Cl}/P_{Na} = 0$ and the dotted lines using Eq. (4) with $P_{Cl}/P_{Na} = 0.21$ for 50 mM and $= 0.13$ for 100 mM NaCl (external concentration). Values of NaCl activities were substituted in the equations for all theoretical predictions.

the physical structure of ion channels. Permeation studies on neuronal and muscle acetylcholine receptor channels have shown that cations bind within the pore and, therefore, do not move through the channel independently (Lewis, 1979; Dwyer, Adams & Hille, 1980; Adams et al., 1981; Sanchez et al., 1986). It has also been shown that the concentration dependence of the single-channel conductance levels off at higher concentrations as if one or more sites become saturated (Dani & Eisenman, 1987). The channels exhibiting a monotonic fall in conductance theoretically indicate that there is single occupancy of sites directly along the permeation pathway (Levitt, 1986). The conductance of a multi-occupied channel would be expected to have an anomalous mole-fraction relationship: with a maximum or minimum in the conductance at one particular mole fraction (Neher, 1975; Hille, 1992). The strongest evidence about the number of binding sites along the permeation pathway is obtained from the concentration dependence of the permeability ratio (Levitt, 1986). The permeability ratio of the muscle nAChR has been shown to be independent of concentration over a wide range, indicating that there is a single occupancy (Dani, 1989). Preliminary rate theory modelling (P.H. Barry, *unpublished calculations*) of our results for the olfactory CNG channels, which have been shown to be similar in organic cation permeation to the ACh end plate channels (Balasubramanian et al., 1995), suggest that the CNG channel possesses more than one ion-binding site in the pore.

There have been a number of studies on cation permeation through photoreceptor cGMP-gated channels on both rods and cones. To characterize ionic permeation

Table 1. Dissociation constants (K_m) and Hill coefficients (h)

Concentration of $[Na^+]_o$ (mM)	At + 50 mV		At − 50 mV	
	K_m (mM)	h	K_m (mM)	h
50	139	3.1	152	3.1
100	149	4.2	144.6	3.4
150	124	4.7	126	3.4
200	112.6	11	109	5.8
250	147	1.5	60	3.6

K_m and h were calculated using the averaged results of normalized currents at +50 mV and −50 mV, through the CNG channels in inside-out dendritic knob patches from olfactory receptor neurons, recorded in each case when various concentrations of NaCl were used to bathe the outside membrane surface. The parameters are those that were used to fit the data points in Fig. 5 *A–F*. Details of the composition of solutions used in the experiments are given in Materials and Methods.

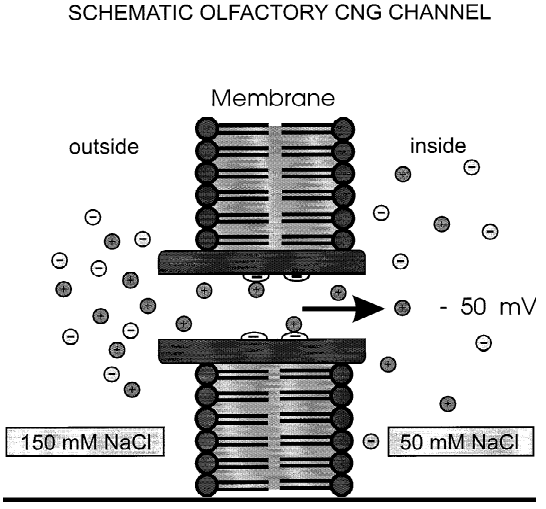

Fig. 8. A schematic representation of the olfactory cAMP-activated channel showing cation permeation at −50 mV with 150 mM NaCl at the outside surface and 50 mM NaCl at the inside surface of the membrane. Preliminary rate theory modelling (P.H. Barry, *unpublished calculations*) suggested that the cations bind to sites within the channel and that these binding sites are located close to the midway point along the channel.

through cyclic nucleotide-activated channels the current and permeability ratios as a function of cation concentration were studied in the photoreceptor CNG channels of retinal rods and cones (Menini, 1990; Zimmerman & Baylor, 1992; Picones & Korenbrot, 1992; Haynes, 1995). The results were consistent with a description of these (CNG) channels as simple ion pores with a high-field-strength-binding site. However Furman & Tanaka (1990) suggested a multi-ion model for these channels and more recently Sesti et al. (1995) have presented evidence for the multi-ion nature of photoreceptor CNG channels. Previous results on the olfactory CNG channels studying the cation selectivity sequence indicated high-field-strength-binding sites (Frings, Lynch & Lindemann, 1992; Balasubramanian et al., 1995) in the olfactory CNG channel. Now the results of this study are also consistent with multiple binding sites for the ions in the channel (Fig. 8). The insensitivity to voltage in asymmetric solutions and the concentration dependence of the data presented in this paper would seem to suggest that these binding sites are most likely to be situated close to the midway point along the channel.

A multi-ion permeation mechanism has been implicated in neuronal background chloride channels (Franciolini & Nonner, 1994) which showed considerable cation permeation through these channels in the presence of permeant anions. In this study, olfactory CNG channels, though purely cation selective under physiological concentrations of NaCl without added divalents, become permeable to chloride ions in very low [NaCl] solutions.

References

Adams, D.J., Nonner, W., Dwyer, T.M., Hille, B. 1981. Block of endplate channels by permeant cations in frog skeletal muscle. *J. Gen. Physiol.* **78:**593–615

Balasubramanian, S., Lynch, J.W., Barry, P.H. 1995. The permeation of organic cations through cAMP-gated channels in mammalian olfactory receptor neurons. *J. Membrane Biol.* **146:**177–191

Balasubramanian, S., Lynch, J.W., Barry, P.H. 1996. Cation interactions within cAMP-activated channels of mammalian olfactory receptor neurons. *Proc. Aust. Physiol. Pharmacol. Soc.* **27:**64P

Barry, P.H., Gage, P.W. 1984. Ionic selectivity of channels at the end plate. *Curr. Top. Membr. Transp.* **21:**1–51

Barry, P.H. 1994. JPCalc, a software package for calculating liquid junction potential corrections in patch-clamp, intracellular, epithelial and bilayer measurements and for correcting junction potential measurements. *J. Neurosci. Methods* **51:**107–116

Boekhoff, I., Tareilus, E., Strotmann, J., Breer, H. 1990. Rapid activation of alternate second messenger pathways in olfactory cilia from rats by different odorants. *EMBO J.* **9:**2453–2458

Dani, J.A., Eisenman, G. 1987. Monovalent and divalent cation permeation in acetylcholine receptor channels: ion transport related to structure. *J. Gen. Physiol.* **89:**959–983

Dani, J.A. 1989. Open channel structure and ion binding sites of the nicotinic acetylcholine receptor channel. *J. Neurosci.* **9:**882–890

Dwyer, T.M., Adams, D.J., Hille, B. 1980. The permeability of the endplate channel to organic cations in frog muscle. *J. Gen. Physiol.* **75:**469–492

Finn, J.T., Grunwald, M.E., Yau, K-W. 1996. Cyclic nucleotide-gated ion channels: An extended family with diverse functions. *Annu. Rev. Physiol.* **58:**395–426

Firestein, S., Zufall, F., Shepherd, G.M. 1991. Single odor sensitive channels in olfactory receptor neurons are also gated by cyclic nucleotides. *J. Neurosci.* **11:**3565–3572

Frings, S., Lynch, J.W., Lindemann, B. 1992. Properties of cyclic nucleotide-gated channels mediating olfactory transduction: activation, selectivity and blockage. *J. Gen. Physiol.* **100:**45–67

Franciolini, F., Nonner, W. 1994. A multi-ion permeation mechanism in neuronal background chloride channels. *J. Gen. Physiol.* **104:**725–746

Furman, R.E., Tanaka, J.C. 1990. Monovalent selectivity of the cyclic

guanosine monophosphate-activated ion channel. *J. Gen. Physiol.* **96:**57–82

Goulding, E.H., Tibbs, G.R., Liu, D., Siegalbaum, S.A. 1993. Role of H5 domain in determining pore diameter and ion permeation through cyclic nucleotide-gated channels. *Nature* **364:**61–64

Hamill, O.P., Marty, A., Neher, E., Sakmann, B., Sigworth, F.J. 1981. Improved patch-clamp techniques for high resolution current recording from cells and cell-free membrane patches. *Pfluegers. Arch.* **391:**85–100

Haynes, L.W. 1995. Permeation of internal and external monovalent cations through the catfish cone photoreceptor cGMP-gated channel. *J. Gen. Physiol.* **106:**485–505

Hille, B. 1992. Ionic Channels of Excitable Membranes. Sinauer Associates, Sunderland, MA

Hodgkin, A.L., Huxley, A.F. 1952. Currents carried by sodium and potassium ions through the membrane of the giant axon of *Loligo. J. Physiol.* **166:**449–472

Kaupp, U.B. 1991. The cyclic nucleotide-gated channels of vertebrate photoreceptors and olfactory epithelium. *Trends in Neurosciences* **14:**150–157

Kurahashi, T., Kaneko, A. 1993. Gating properties of the cAMP-gated channel in toad olfactory receptor cells. *J. Physiol.* **466:**287–302

Lewis, C.A. 1979. Ion-concentration dependence of the reversal potential and the single channel conductance of ion channels at the frog neuromuscular junction. *J. Physiol.* **286:**417–455

Levitt, D.G. 1986. Interpretation of biology ion channel flux data: reaction-rate versus continuum theory. *Ann. Rev. Biophys. Biophys. Chem.* **15:**29–57

Lynch, J.W., Barry, P.H. 1991. Properties of transient K^+ currents and underlying single K^+ channels in rat olfactory receptor neurons. *J. Gen. Physiol.* **97:**1043–1072

Menini, A. 1990. Currents carried by monovalent cations through cyclic GMP-activated channels in excised patches from salamander rods. *J. Physiol.* **424:**167–185

Nakamura, T., Gold, G.H. 1987. A cyclic nucleotide-gated conductance in olfactory receptor cilia. *Nature* **325:**442–444

Neher, E. 1975. Ionic specificity of the gramicidin channel and the thallous ion. *Biochim. Biophys. Acta* **401:**540–544

Picones, A., Korenbrot, J.L. 1992. Permeation and interaction of monovalent cations with the cGMP-gated channel of cone photoreceptors. *J. Gen. Physiol.* **100:**647–673

Reed, R.R. 1992. Signalling pathways in odorant detection. *Neuron* **8:**205–209

Robinson, R.A., Stokes, R.H. 1965. *Electrolyte Solutions*, 2nd edition (revised), p. 479. Butterworth Ltd., London

Ronnett, G.V., Cho, H., Hester, L.D., Wood, S.F., Snyder, S.H. 1993. Odorants differentially enhance phophoinositide turnover and adenyl cyclase in olfactory receptor neuronal cultures. J. Neurosci. **13:**1751–1758

Ruff, R.L. 1986. Ionic channels: I. The biophysical basis for ion passage and channel gating. *Muscle & Nerve* **9:**675–699

Sanchez, J.A., Dani, J.A., Siemen, D., Hille, B. 1986. Slow permeation of organic cations in acetylcholine receptor channels. *J. Gen. Physiol.* **87:**985–1001

Sesti, F., Eismann, E., Kaupp, U.B., Nizzari, M., Torre, V. 1996. The multi-ion nature of the cGMP-gated channel from vertebrate rods. *J. Physiol.* **487:**17–36

Zimmerman, A.L., Baylor, D.A. 1992. Cation interactions within the cyclic GMP-activated channel of retinal rods from the tiger salamander. *J. Physiol.* **449:**759–783

Zufall, F., Firestein, S., Shepherd, G.M. 1991. Analysis of single cyclic-nucleotide-gated channels in olfactory receptor cells. . *Neurosci.* **11:**3573–3580